Lead-supported Germanium Nanowire Growth

Michael S. Seifner,[a,†] Patrik Pertl,[a,†] Johannes Bernardi,[b] Subhajit Biswas,[c,d] Justin D. Holmes[c,d] and Sven Barth[a,]*

[a] Vienna University of Technology, Institute of Materials Chemistry, Getreidemarkt 9/BC/02, 1060 Vienna, Austria.

[b] University Servicecenter for TEM (USTEM), Vienna University of Technology, Wiedner Hauptstrasse 8-10, 1040 Vienna, Austria.

[c] Materials and Supercritical Fluids Group, Department of Chemistry and the Tyndall National Institute, University College Cork, Cork, Ireland.

[d] Centre for Research on Adaptive Nanostructures and Nanodevices (CRANN), Trinity College Dublin, Dublin 2, Ireland.

[†] MSS and PP contributed equally to this study.

* Corresponding author: sven.barth@tuwien.ac.at

Keywords: Germanium; Lead; Nanowire; Growth

Abstract

The Pb-assisted growth of Ge nanowires (NWs) has been investigated under high and low pressure conditions via thermal decomposition of diphenylgermane. Highly crystalline Ge NWs were obtained and Pb was established as a viable growth promoter with the Pb particle being in the solid and liquid state.

Introduction

One-dimensional semiconductors such as nanotubes, and nanowires offer exciting possibilities for future high-density electronic circuits, sensing, nanophotonics, energy harvesting and storage applications [1]. Germanium is a particularly interesting semiconductor due to its high hole mobility and the potential of a transition from an indirect to a direct bandgap material upon straining [2]. In addition, the use of Ge NW meshes as viable anode material for lithium ion batteries has shown promising results [3].

Ge NWs are usually grown via metal-assisted processes using different metal growth promoters including transition metals Au [4], Ag [5], Ni [6], Cu [7], Mn [8], Ir [9], Co [9], Fe [9], and main group metals Al [10], Sn [11], Bi [12] as well as In [13]. Moreover, FePt [9], $MnPt_3$ [9], AlAu [14] and AgAu [15] alloys are also used to promote Ge NW growth via gas-phase reactions. For electronic applications the potential incorporation of the metal seed material in the semiconductor NW has to be taken into account [16], because deep level traps can significantly alter the electronic properties [17]. However, in exceptional cases the incorporation of the seeding material is desired to form metastable material compositions such as GeSn alloys [18, 19]. Typically, Sn and Pb do not lead to deep level traps in Ge, which makes these seeds particularly interesting for the Ge NW growth [20]. While Sn seeds have been used in vapour-phase Ge NW growth processes [21] and in the solution-based synthesis for the formation of Ge NWs as well as nanorods [22], Pb has not been described to be a viable growth promoter for Ge NWs to date.

Following the classification by Schmidt *et al.*, Pb is a type B growth promoter with a eutectic containing less than 1 % of the semiconductor material and the absence of germanides [23]. The phase diagram reveals 0.07 % Ge in the eutectic with a melting point of 327.5 °C [24]. As a consequence, Pb may act as an alternative growth promoter for the formation of axial heterostructures with sharp interfaces due to the extremely low solubility of the semiconductor material and the associated negligible reservoir effect [25]. The similarity of the phase diagram to the Sn/Ge system already suggests a potentially similar behaviour in these alternating growth processes targeting segmented nanostructures.

Here we report the Pb-supported Ge NW growth via supercritical-fluid synthesis as well as low pressure CVD. The growth procedures have been performed above and below the eutectic temperature in the Ge/Pb system. The results suggest that the growth can proceed via the vapour-liquid-solid (VLS) [26] and the related supercritical fluid-liquid-solid (SFLS) [27] mechanism as well as from solid seeds representing the supercritical fluid-solid-solid (SFSS) growth mode [28].

Experimental section

The growth was typically performed in batch reactions in supercritical toluene and also via low pressure CVD using diphenylgermane (DPG) as precursor at temperatures of 340-430 °C. DPG was used before for Ge NW formation in both aforementioned growth strategies using different growth seeds [29, 30]. The detailed growth conditions are described in the Supplementary Information. In addition, operators should be aware of the toxicity of Pb-containing materials and compounds.

Results and discussion

Typical scanning electron micrographs show the formation of Ge NWs in high density when grown at temperatures of higher than 380 °C by SFLS and VLS (Fig. 1a+b). Usually the Ge NW density is higher in the solvent-based synthesis procedures, which could be caused by the exclusive handling of the growth promoters under inert atmospheres in a glove box. In contrast, silicon substrates containing Pb growth seeds have been transferred to the CVD growth chamber under ambient atmospheres. This transport might have caused oxidation/deactivation of the metal particles resulting in lower Ge NW density. A clear indication of the metal supported growth via the VLS/SFLS mechanism is provided in TEM and SEM images showing the termination of each wire with a metal particle. For instance, Fig. S1 in the Supplementary Information shows the formation of short NWs terminated with hemispherical particles.

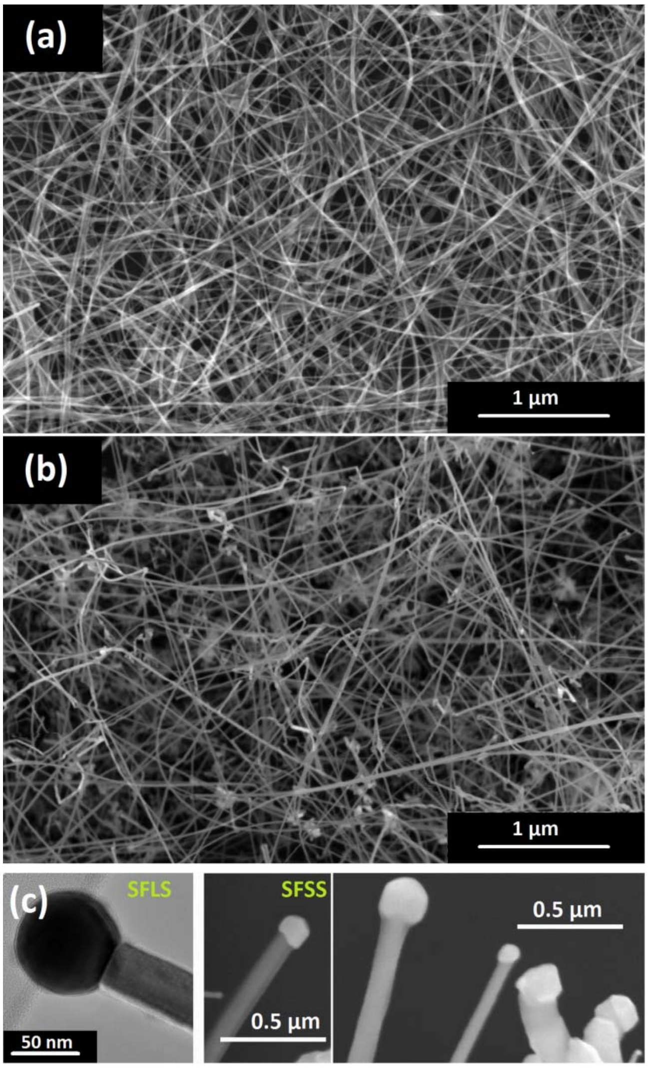

Fig. 1 *The SEM images show Ge NWs grown in (a) supercritical toluene at 380 °C with a reactor pressure of 320 bar and (b) by low pressure CVD at 430 °C at 10^{-2} mbar using DPG as precursor. (c) shows the observed shapes of the metal particle associated with a liquid growth promoter (SFLS mechanism; T>340°C) and solid seeds (SFSS mechanism; T=250 °C).*

Ge NWs are also formed approx. 80 °C below the eutectic temperature in the supercritical fluid system at 250 °C. Testing this growth regime requires a change in growth strategy, which includes the use of Pb and Ge imides as precursors. DPG does not decompose sufficiently at these temperatures and therefore the change in precursor species is necessary. The density of the Ge NWs grown at these reduced temperatures is much lower and kinking is more pronounced when compared to NWs grown at temperatures above the eutectic (Fig. S2).

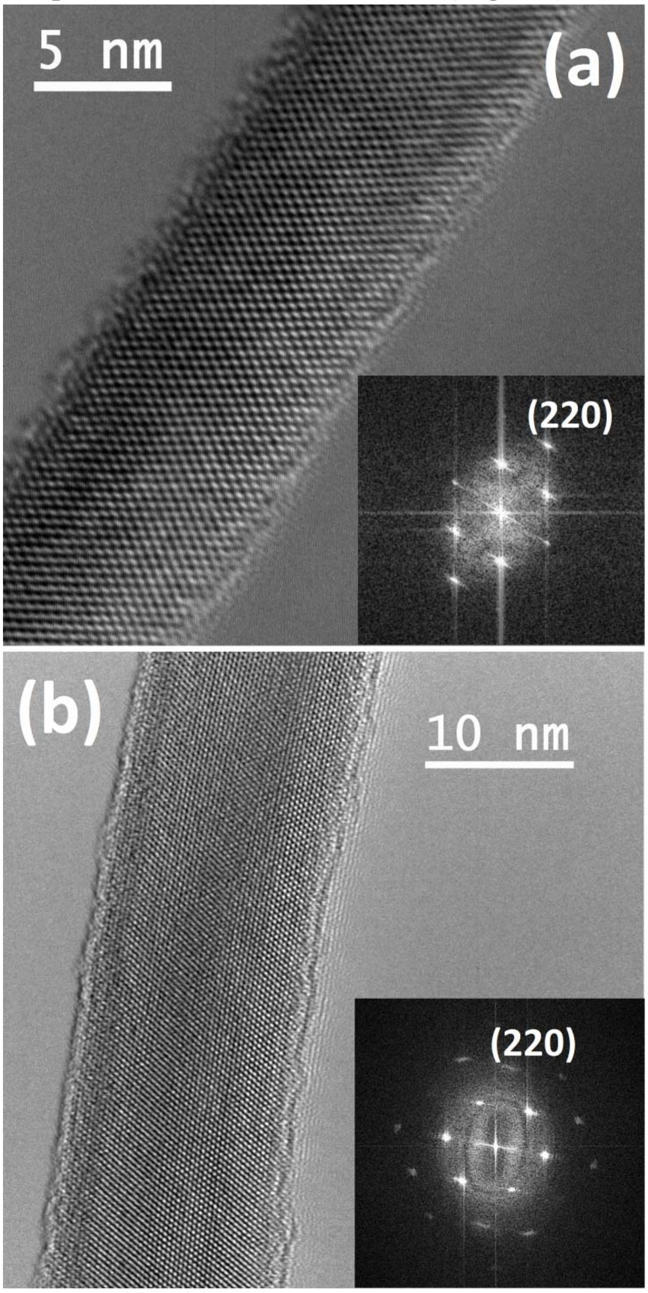

Fig. 2 *The HRTEM in the inset and the corresponding FFT pattern also illustrate the high crystallinity of the Ge NWs grown (a) at 380°C in supercritical toluene and (b) at 430 °C by low pressure CVD. The insets show the* ⟨011⟩ *growth direction of the* Ge NWs.

SEM images in Fig. 1(c) show the non-hemispherical metal particles typical for the SFSS mechanism at low temperatures. In contrast, the shape of molten particles typical for SFLS/VLS growth at temperatures above the eutectic is illustrated in the TEM image. Differences in the composition between the NW body and the terminating particle are represented by the different brightness of the two components due to the Z-contrast. The possibility to grow NWs from the same seed material in either solid or molten state has been already demonstrated for Au nanoparticles by lowering the growth temperatures during in situ imaging [4]. In addition, growth of Ge NWs on Pb bulk substrates has been investigated in a supercritical batch process to complement the studies using Pb particles. Fig. S3 shows clearly the formation of Ge NWs from those bulk substrates close to the eutectic temperature (320 °C).

The Pb-seeded Ge NWs have been characterised by transmission electron microscopy (TEM). Fig. 2 shows TEM images of highly crystalline Pb-seeded Ge NWs. According to the TEM images and the corresponding fast Fourier transform (FFT) pattern, the growth of the majority of Ge NWs proceeds along the ⟨011⟩ axis and a smaller fraction of ⟨111⟩-oriented NWs is observed. The high number of ⟨011⟩-oriented Ge NWs is probably caused by the diameter of the majority (>90°%) of the NWs (10-25 nm), which is known to result in a higher number of group 14 NWs with ⟨011⟩ growth direction for diameters below 20 nm [31, 32]. The small radial dimensions and more examples of high resolution TEM images in Fig. S4 and S5 of the Supplementary Information.

The local Pb concentration in the *Ge* NWs has been evaluated using energy dispersive X-ray spectroscopy (EDX) elemental mapping. Fig. 3 shows a bright field TEM image of a Ge NW with the metal particle at the tip as well as scanning transmission electron microscopy (STEM)-EDX mapping for Pb and Ge. The Pb signal is confined to the tip region and the NW body contains exclusively Ge. These results could be expected from the phase diagram of the immiscible Ge and Pb components; however, we cannot rule out the incorporation of very small Pb concentrations using EDX analysis. Recently, a rare report described up to 0.2 % Pb at substitutional sites for a crystallised, thin GePb layer prepared by laser ablation;

nevertheless these metastable phases usually require kinetic instead of thermodynamic control of the formation process [33].

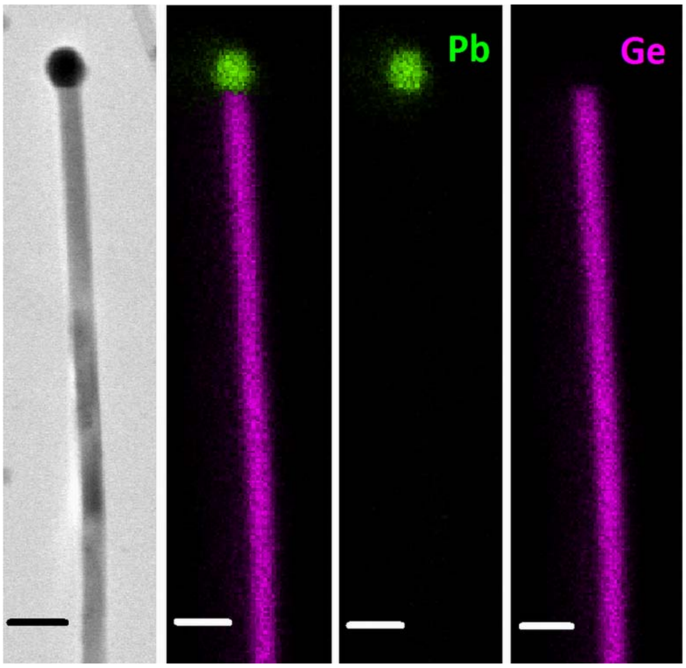

Fig. 3 *Bright field TEM image and EDX mapping with Pb (green) and Ge (purple) displayed together and individually. The scale bars are 50 nm in each image.*

Conclusions

The potential of Pb to act as growth seed for Ge NWs has been demonstrated under supercritical conditions and by low pressure CVD. SFSS and SFLS/VLS growth regimes are observed and associated with solid Pb seeds and molten particles. These investigations on the previously not described Pb-seeding of Ge NWs could be used for the formation of group 14 semiconductor heterostructures with sharp interfaces due to the low solubility of the semiconductor in the seed particle and the activity of Pb to promote Si NW growth described in literature [34].

Acknowledgements

This study was supported by TU Vienna research funds. JDH acknowledges funding from the Science Foundation Ireland (Grant No.: 14/IA/2513).

References

[1] S. Barth, F. Hernandez-Ramirez, J.D. Holmes, A. Romano-Rodriguez, Prog. Mater. Sci., 55 (2010) 563-627.
[2] J.R. Sánchez-Pérez, C. Boztug, F. Chen, F.F. Sudradjat, D.M. Paskiewicz, R. Jacobson, M.G. Lagally, R. Paiella, Proc. Nat. Acad. Sci. U.S.A., 108 (2011) 18893-18898.
[3] T. Kennedy, E. Mullane, H. Geaney, M. Osiak, C. O'Dwyer, K.M. Ryan, Nano Lett., 14 (2014) 716-723.
[4] S. Kodambaka, J. Tersoff, M.C. Reuter, F.M. Ross, Science, 316 (2007) 729-732.
[5] S. Barth, J.J. Boland, J.D. Holmes, Nano Lett., 11 (2011) 1550-1555.
[6] S. Barth, M.M. Koleśnik, K. Donegan, V. Krstić, J.D. Holmes, Chem. Mater., 23 (2011) 3335-3340.
[7] H. Geaney, C. Dickinson, C.A. Barrett, K.M. Ryan, Chem. Mater., 23 (2011) 4838-4843.
[8] J.L. Lensch-Falk, E.R. Hemesath, F.J. Lopez, L.J. Lauhon, J. Am. Chem. Soc., 129 (2007) 10670-10671.
[9] H.Y. Tuan, D.C. Lee, B.A. Korgel, Angew. Chem.-Int. Edit., 45 (2006) 5184-5187.
[10] B.T. Richards, B. Gaskey, B.D.A. Levin, K. Whitham, D. Muller, T. Hanrath, J. Mater. Chem. C, 2 (2014) 1869-1878.
[11] H. Geaney, E. Mullane, Q.M. Ramasse, K.M. Ryan, Nano Lett., 13 (2013) 1675-1680.
[12] X. Lu, D.D. Fanfair, K.P. Johnston, B.A. Korgel, J. Am. Chem. Soc., 127 (2005) 15718-15719.
[13] J. Park, K. Kim, Electron. Mater. Lett., 8 (2012) 545-548.
[14] C.-Y. Wen, M.C. Reuter, J. Bruley, J. Tersoff, S. Kodambaka, E.A. Stach, F.M. Ross, Science, 326 (2009) 1247-1250.
[15] C. O'Regan, S. Biswas, S. Barth, M.A. Morris, N. Petkov, J.D. Holmes, J. Mater. Chem. C, 2 (2014) 4597-4605.
[16] J.E. Allen, E.R. Hemesath, D.E. Perea, J.L. Lensch-Falk, Z.Y. Li, F. Yin, M.H. Gass, P. Wang, A.L. Bleloch, R.E. Palmer, L.J. Lauhon, Nat. Nanotechnol., 3 (2008) 168-173.
[17] E. Koren, G. Elias, A. Boag, E.R. Hemesath, L.J. Lauhon, Y. Rosenwaks, Nano Lett., 11 (2011) 2499-2502.
[18] S. Barth, M.S. Seifner, J. Bernardi, Chem. Commun., 51 (2015) 12282-12285.
[19] M.S. Seifner, F. Biegger, A. Lugstein, J. Bernardi, S. Barth, Chem. Mater., 27 (2015) 6125-6130.
[20] W.W. Tyler, J. Phys. Chem. Solids, 8 (1959) 59-65.
[21] E. Mullane, T. Kennedy, H. Geaney, C. Dickinson, K.M. Ryan, Chem. Mater., 25 (2013) 1816-1822.
[22] X. Lu, B.A. Korgel, Chem. Eur. J., 20 (2014) 5874-5879.
[23] V. Schmidt, J.V. Wittemann, S. Senz, U. Gosele, Adv. Mater., 21 (2009) 2681-2702.
[24] R.W. Olesinski, G.J. Abbaschian, Bull. Alloy Phase Diagr., 5 (1984) 374-377.
[25] G. Flynn, Q.M. Ramasse, K.M. Ryan, Nano Lett., (2015).
[26] R.S. Wagner, W.C. Ellis, Appl. Phys. Lett., 4 (1964) 89-90.
[27] J.D. Holmes, K.P. Johnston, R.C. Doty, B.A. Korgel, Science, 287 (2000) 1471-1473.
[28] H.Y. Tuan, D.C. Lee, T. Hanrath, B.A. Korgel, Chem. Mater., 17 (2005) 5705-5711.
[29] T. Hanrath, B.A. Korgel, J. Am. Chem. Soc., 124 (2002) 1424-1429.
[30] S. Barth, R. Jimenez-Diaz, J. Sama, J.D. Prades, I. Gracia, J. Santander, C. Cane, A. Romano-Rodriguez, Chem. Commun., 48 (2012) 4734-4736.
[31] V. Schmidt, S. Senz, U. Gosele, Nano Lett., 5 (2005) 931-935.
[32] R.G. Hobbs, S. Barth, N. Petkov, M. Zirngast, C. Marschner, M.A. Morris, J.D. Holmes, J. Am. Chem. Soc., 132 (2010) 13742-13749.
[33] Q. Zhou, T.K. Chan, S.L. Lim, C. Zhan, T. Osipowicz, X. Gong, E.S. Tok, Y.-C. Yeo, ECS Solid State Lett., 3 (2014) P91-P93.
[34] F.-W. Yuan, H.-J. Yang, H.-Y. Tuan, J. Mater. Chem. C, 21 (2011) 13793-13800.